

Hydrodynamical transport of angular momentum in accretion disks in the presence of nonlinear perturbations due to noise

Subham Ghosh* and Banibrata Mukhopadhyay†

*Department of Physics, Indian Institute of Science,
Bangalore, Karnataka, 560012, India*

**subham@iisc.ac.in*

†*bm@iisc.ac.in*

The origin of hydrodynamical instability and turbulence in the Keplerian accretion disk is a long-standing puzzle. The flow therein is linearly stable. Here we explore the evolution of perturbation in this flow in the presence of an additional force. Such a force, which is expected to be stochastic in nature hence behaving as noise, could result from thermal fluctuations (however small be), grain–fluid interactions, feedback from outflows in astrophysical disks, etc. We essentially establish the evolution of nonlinear perturbation in the presence of Coriolis and external forces, which is the modified Landau equation. We obtain that even in the linear regime, under suitable forcing and Reynolds number, the otherwise least stable perturbation evolves to a very large saturated amplitude, leading to nonlinearity and plausible turbulence. Hence, forcing essentially leads a linear stable mode to unstable. We further show that nonlinear perturbation diverges at a shorter time-scale in the presence of force, leading to a fast transition to turbulence. Interestingly, the emergence of nonlinearity depends only on the force but not on the initial amplitude of perturbation, unlike the original Landau equation-based solution.

Keywords: accretion, accretion disks – hydrodynamics – instabilities – turbulence

1. Introduction

Origin of instability and plausible turbulence in Rayleigh stable flows, e.g., the Keplerian accretion flow, is a long-standing problem. While such flows are evident to be turbulent, they are linearly stable for any Reynolds number (Re). Although people^{1,2} described the underlying flow in accretion disks to be turbulent with an effective turbulent viscosity, the origin of turbulence therein was not clear until Balbus and Hawley³ proposed the idea of magnetorotational instability (MRI) following Velikhov⁴ and Chandrasekhar⁵. MRI is a Magnetohydrodynamical (MHD) instability, and it operates due to the coupling between the weak magnetic field and the rotation of the fluid parcel. Although MRI is a popular instability mechanism, it poses several problems. There are astrophysical bodies where the ionization fraction is tiny as they are cold. In such systems, MRI gets suppressed⁶. Apart from that, beyond a certain value of the toroidal component of the magnetic field for compressible plasma, MRI gets suppressed^{7,8}. There are several other cites too where MRI seizes to work or becomes suppressed^{9,10}. We, therefore, venture for a hydrodynamical origin of nonlinearity and hence plausible turbulence in the accretion disk. Our emphasis is the conventional linear instability when perturbation grows exponentially, unlike the case of transient growth. We particularly consider

2

here an extra force¹¹, to fulfill our purpose. The examples¹² of the origin of such force in astrophysical context, particularly in accretion disks, could be: the interaction between the dust grains and fluid parcel in protoplanetary disks, back reactions of outflow/jet to accretion disks.

2. Formalism of the problem

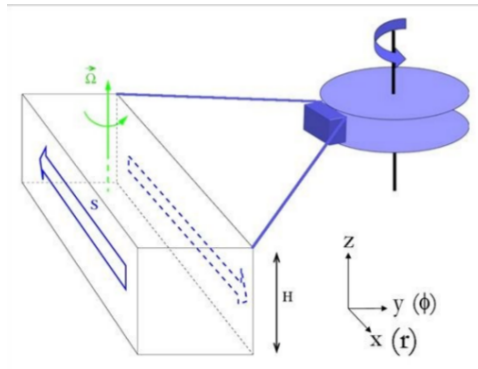


Fig. 1. Model picture of local cubical box in accretion disk where we perform the analysis (<http://ipag.obs.ujf-grenoble.fr/~longarep/astrophysics.html>). Within the box, the Cartesian coordinate x is along the radial cylindrical coordinate r (with respect to the center of the accretion disk), y is along ϕ , and z is same in both the systems.

To formulate the problem, we have considered a local box at a local patch in the accretion disk, as shown in the Fig. 1. Although the accretion disk possesses cylindrical geometry, In the local box, we study the motion of the local fluid element using the Cartesian coordinates. The one to one correspondence between the Cartesian (x, y, z) and cylindrical (r, ϕ, z) coordinates are shown in the Fig. 1. The Cartesian coordinates x, y, z are along the cylindrical coordinates r, ϕ, z . The details of the local formulation are in Mukhopadhyay et al.^{13,14}, and Ghosh and Mukhopadhyay¹⁵. As we confine ourselves in the local region of the accretion disks, the corresponding flow has been considered incompressible^{9,13,16-18}. The governing equations are the ensemble-averaged Orr-Sommerfeld and Squire equations in the presence of Coriolis force and an additional stochastic force^{12,19}, which is delta correlated with nonzero mean. The Orr-Sommerfeld and Squire equations are obtained by eliminating the pressure term from the corresponding Navier-Stokes equations and utilizing the continuity equation for the incompressible flow. The governing equations are given by,

$$\left(\frac{\partial}{\partial t} + U \frac{\partial}{\partial y} \right) \nabla^2 u - U'' \frac{\partial u}{\partial y} + \frac{2}{q} \frac{\partial \zeta}{\partial z} - \frac{1}{Re} \nabla^4 u + \Gamma_1 = NL^u, \quad (1)$$

$$\left(\frac{\partial}{\partial t} + U \frac{\partial}{\partial y}\right) \zeta - U' \frac{\partial u}{\partial z} - \frac{2}{q} \frac{\partial u}{\partial z} - \frac{1}{Re} \nabla^2 \zeta + \Gamma_2 = NL^\zeta, \quad (2)$$

where u and ζ are respectively the x -component of the velocity and vorticity perturbations after ensemble averaging, U the y -component of background velocity which for the present purpose of plane shear in the dimensionless units is $-x$, q the rotation parameter with $\Omega(r) \propto 1/r^q$, $\Omega(r)$ being the angular frequency of the fluid parcel at radius r , Γ -s are the corresponding constant means of stochastic forces (white noise with nonzero mean due to gravity making the system biased¹¹) in the system described below, and NL -s are the non-linear terms due to the perturbation. The x -component of vorticity and the non-linear terms are given by

$$\zeta = \frac{\partial w}{\partial y} - \frac{\partial v}{\partial z}, \quad (3)$$

$$NL^u = -\nabla^2 \{(\mathbf{u}' \cdot \nabla)u\} + \frac{\partial}{\partial x} \nabla \cdot \{(\mathbf{u}' \cdot \nabla)\mathbf{u}'\}, \quad (4)$$

$$NL^\zeta = -\frac{\partial}{\partial y} \{(\mathbf{u}' \cdot \nabla)w\} + \frac{\partial}{\partial z} \{(\mathbf{u}' \cdot \nabla)v\}, \quad (5)$$

where $\mathbf{u}' = (u, v, w)$, which is the perturbed velocity vector. For the complete description of the flow, equations 1 and 2 are supplemented with the equation of continuity, which is given by

$$\nabla \cdot \mathbf{u}' = 0, \quad (6)$$

To solve the governing equations, we have no-slip boundary conditions along x -direction^{12,13,20}, i.e. $u = v = w = 0$ at $x = \pm 1$ or equivalently

$$u = \frac{\partial u}{\partial x} = \zeta = 0, \quad \text{at } x = \pm 1. \quad (7)$$

2.1. Linear Theory

In the evolution of linear perturbation, let the linear solutions be

$$u = \hat{u}(x, t)e^{i\mathbf{k} \cdot \mathbf{r}}, \quad (8)$$

$$\zeta = \hat{\zeta}(x, t)e^{i\mathbf{k} \cdot \mathbf{r}}, \quad (9)$$

with $\mathbf{k} = (0, k_y, k_z)$ and $\mathbf{r} = (0, y, z)$. Substitute these in equations (1) and (2), neglecting non-linear terms, we obtain

$$\frac{\partial}{\partial t} Q + i\mathcal{L}Q + \Gamma = 0, \quad (10)$$

where

$$Q = \begin{pmatrix} \hat{u} \\ \hat{\zeta} \end{pmatrix}, \quad \mathcal{L} = \begin{pmatrix} \mathcal{L}_{11} & \mathcal{L}_{12} \\ \mathcal{L}_{21} & \mathcal{L}_{22} \end{pmatrix}, \quad \mathcal{D} = \frac{\partial}{\partial x}, \quad (11)$$

4

$$\begin{aligned}\mathcal{L}_{11} &= (\mathcal{D}^2 - k^2)^{-1} \left[k_y U (\mathcal{D}^2 - k^2) - k_y U'' - \frac{1}{iRe} (\mathcal{D}^2 - k^2)^2 \right], \\ \mathcal{L}_{12} &= (\mathcal{D}^2 - k^2)^{-1} \frac{2k_z}{q}, \\ \mathcal{L}_{21} &= - \left(U' + \frac{2}{q} \right) k_z, \\ \mathcal{L}_{22} &= k_y U - \frac{1}{iRe} (\mathcal{D}^2 - k^2),\end{aligned}$$

and

$$\Gamma = e^{-i\mathbf{k}\cdot\mathbf{r}} \begin{pmatrix} (\mathcal{D}^2 - k^2)^{-1} \Gamma_1 \\ \Gamma_2 \end{pmatrix}. \quad (12)$$

Let us subsequently assume the trial solution of the equation (10) be

$$Q = A Q_x e^{-i\sigma t} - \frac{1}{\mathcal{D}_t + i\mathcal{L}} \Gamma, \quad (13)$$

where σ is the eigenvalue corresponding to the particular mode and it is complex having real (σ_r) and imaginary (σ_i) parts,

$$Q_x = \begin{pmatrix} \phi^u(x) \\ \phi^\zeta(x) \end{pmatrix} \quad (14)$$

and \mathcal{D}_t stands for $\partial/\partial t$. Q_x is the eigenfunction corresponding to the homogeneous part of the equation (10), i.e., Q_x satisfies $\mathcal{L}Q_x = \sigma Q_x$. The first term of the right-hand side of the equation (13) is due to the homogeneous part of the equation (10), and the second term is due to the inhomogeneous part, i.e., the presence of Γ , of the same equation. Hence, Q is influenced by the force Γ . However, the typical eigenspectra for the Keplerian flow ($q = 1.5$), constant angular momentum flow ($q = 2$) and plane Couette flow ($q \rightarrow \infty$) for $Re = 2000$ and $k_y = k_z = 1$ are shown in the Fig. 2. Since \mathcal{L}_{12} and \mathcal{L}_{21} in the equation (11) are zero for the plane Couette flow and constant angular momentum flow, respectively, we obtain the same eigenspectra for both plane Couette, and constant angular momentum flows. We perform the whole analysis for the least stable modes for the respective flows, and these least stable modes are shown in the dotted box in Fig. 2.

2.2. Nonlinear theory

For the non-linear solution, following similar work but in the absence of force^{20–22}, we assume the series solution for velocity and vorticity, i.e.

$$\psi = \sum_{n \rightarrow -\infty}^{\infty} \psi_n = \sum_{n \rightarrow -\infty}^{\infty} \bar{\psi}_n(t, x) e^{in(\mathbf{k}\cdot\mathbf{r} - \sigma_r t)}, \quad (15)$$

when obviously $\bar{\psi}_{-n} = \bar{\psi}_n^*$ and ψ could be any one of u and ζ .

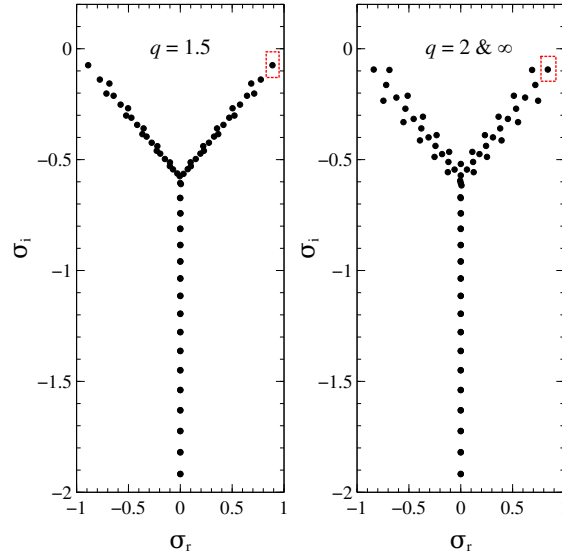


Fig. 2. Variation of σ_i with σ_r for $Re = 2000$ and $k_y = k_z = 1$ for the Keplerian flow ($q = 1.5$), constant angular momentum flow ($q = 2$) and plane Couette flow ($q \rightarrow \infty$). The latter two eigenspectra are identical. The dotted box represents the least stable mode for the respective cases.

We substitute these in equations (1) and (2) and collect the coefficients of the term $e^{i(\mathbf{k}\cdot\mathbf{r}-\sigma_r t)}$, to capture least nonlinear effect following, e.g.,^{12,20,22}, from both sides and obtain

$$\frac{\partial Q_1}{\partial t} - i\sigma_r Q_1 + i\mathcal{L}Q_1 = NL_1, \quad (16)$$

where $NL_1 = \begin{pmatrix} (\mathcal{D}^2 - k^2)^{-1} NL_1^u \\ NL_1^\zeta \end{pmatrix}$ and $Q_1 = \begin{pmatrix} \bar{u}_1(x, t) \\ \bar{\zeta}_1(x, t) \end{pmatrix}$. We assume the solution for Q_1 to be

$$Q_1 = \sum_{m=1}^{\infty} A_{t,m} Q_{x,m} - \frac{1}{\mathcal{D}_t + i\mathcal{L}} \Gamma, \quad (17)$$

where m stands for various eigenmodes.

However, to the first approximation, our interest is in the least stable mode. Similar descriptions in two dimensions²⁰ without Γ and three-dimensional Keplerian disks²² without Γ are already there in the literature and we mostly follow their formalism. We, therefore, omit the summation, and subscript m in the equation (17), and obtain

$$Q_1 = A_t Q_x - \frac{1}{\mathcal{D}_t + i\mathcal{L}} \Gamma. \quad (18)$$

6

We then substitute the equation (18) in the equation (16) and using bi-orthonormality between Q_x and its conjugate function \tilde{Q}_x , we obtain

$$\frac{dA_t}{dt} - \sigma_i A_t + \mathcal{N} = p|A_t|^2 A_t, \quad (19)$$

where

$$\mathcal{N} = \int_{-1}^1 dx \tilde{Q}_x^\dagger \Gamma' \quad (20)$$

and

$$p = \int_{-1}^1 dx \tilde{Q}_x^\dagger \mathcal{S}, \quad (21)$$

where

$$\begin{aligned} \Gamma' &= -\Gamma + i\sigma_r \left(\frac{1}{\mathcal{D}_t + i\mathcal{L}} \right) \Gamma \\ &= -\Gamma + i\sigma_r (t - i\mathcal{L}t^2) (1 + \mathcal{L}^2 t^2)^{-1} \Gamma, \end{aligned} \quad (22)$$

\mathcal{S} is the spatial contribution from the nonlinear terms. For the greater details, see Ghosh and Mukhopadhyay¹².

Throughout the paper, Γ from the equation (12) has been decomposed as $\Gamma \rightarrow \Gamma \begin{pmatrix} 1 \\ 1 \end{pmatrix}$ by adjusting Γ_1 and Γ_2 , as they are only the free parameters.

The evolution of \mathcal{N} has been shown in Fig. 3 for the parameters mentioned in the figure. It shows that \mathcal{N} becomes saturated beyond a certain time, and the saturation depends on Re . As Re increases, the saturation increases. Fig. 4 shows the variation of the least stable (the one in the dotted box in Fig. 2) as a function of Re in the case of the Keplerian flow. It tells us that the least stable mode approaches zero as Re is increased.

3. Results

Equation (19), which is a nonlinear equation, tells us about the evolution of the amplitude of the perturbation. To explore the evolution of linear and nonlinear perturbations, we use the equation (19) accordingly. For the evolution of the linear perturbation, we get rid of the nonlinear term in equation (19).

3.1. Evolution of $|A|_t$ in the linear regime

In the linear regime, the equation (19) becomes

$$\frac{dA_t}{dt} = \sigma_i A_t - \mathcal{N}. \quad (23)$$

This equation tells that at large t , $|A_t|$ becomes $|\mathcal{N}|/|\sigma_i|$ ¹².

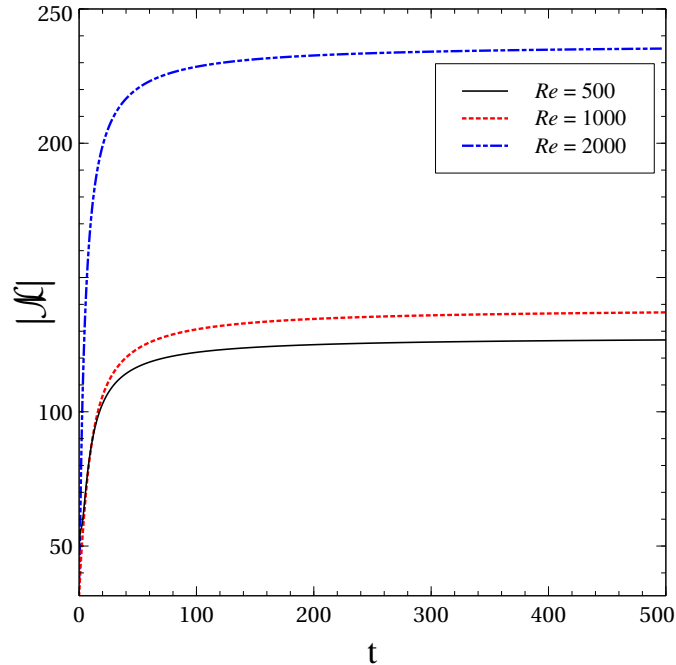


Fig. 3. Variation of \mathcal{N} as a function of t for $Re = 500, 1000$ and 2000 , for $\Gamma = 10^4$ and $k_y = k_z = 1$, corresponding to the respective least stable modes.

Fig. 5 shows the variation of $|A_t|$ as a function of t for various values of Re and Γ . Fig. 5 also suggests the scaling relation between saturated $|A_t|$ and Γ to be

$$|A_t| \propto \Gamma \quad (24)$$

for a fixed Re . Apart from that, we notice that for a fixed Γ , $|A_t|$ becomes saturated at $|\mathcal{N}|/|\sigma_i|$ beyond a certain time, and the saturation increases as Re increases. This saturation is independent of the initial condition¹². This is because at a fixed Γ , $|\mathcal{N}|$ becomes saturated (see Fig. 3) at a fixed value, and the saturated value increases as Re increases, as well as $|\sigma_i|$ increases as Re increases (see Fig. 4). Now, in the accretion disk, Re is huge¹⁹ ($\gtrsim 10^{14}$). The smaller Γ , therefore, can bring nonlinearity in the accretion disk, as for huge Re , $|\sigma_i|$ is infinitesimally small. Hence, $|\mathcal{N}|/|\sigma_i|$ becomes enormous. This huge saturation of $|A_t|$ could bring nonlinearity and hence plausibly turbulence in the underlying Keplerian flow.

3.2. Evolution of $|A_t|$ in the nonlinear regime

In the nonlinear regime, the evolution of $|A_t|$ is described by the equation (19). Fig. 6 describes the variation of $|A_t|$ as a function of t for nonlinear perturbation in the Keplerian flow. In the figure, $RE(A_t)$ and $IM(A_t)$ indicate the real and imaginary parts of initial A_t , respectively. It tells us that for $\Gamma = 0$, depending on

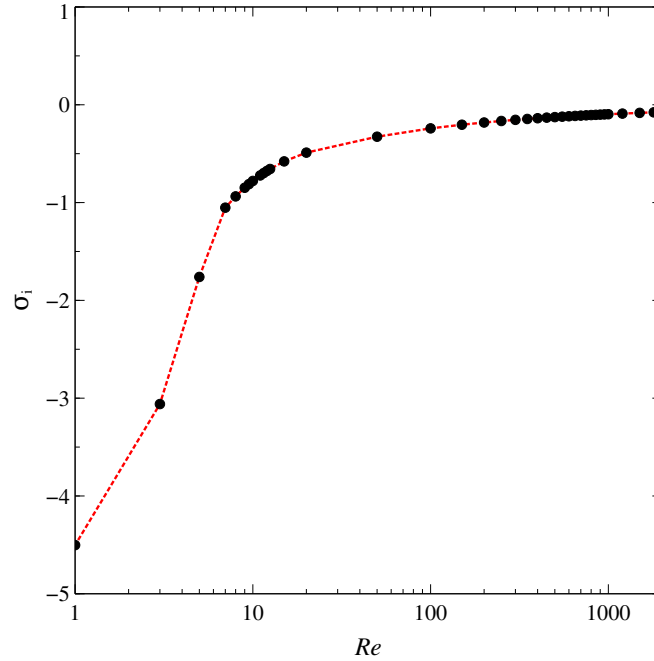


Fig. 4. Variation of the least stable σ_i as a function of Re for $k_y = k_z = 1$ in the Keplerian flow.

the initial amplitude, $|A_t|$ may diverge (green line) or $|A_t|$ may decay (continuous black line) to zero from the initial amplitude. When there is no noise, i.e., $\Gamma = 0$, the diverging solution of $|A_t|$ occurs when the initial amplitude is beyond a critical amplitude¹². It is apparent that the onset of the nonlinearity depends on the initial amplitude of perturbation in the absence of the force, but it does not depend on the same in the presence of force¹². The divergence of $|A_t|$ and hence the onset of nonlinearity and plausible turbulence depends only on the strength of the force, as shown by dashed (magenta) line, compared to dot-dashed (blue) and dotted (red) lines, in Fig. 6.

4. Conclusion

If there is no extra force involved in the system, then the equation (19) becomes the usual Landau equation, which is

$$\frac{dA_t}{dt} = \sigma_i A_t + p|A_t|^2 A_t, \quad (25)$$

which can be further recast to

$$\frac{d|A|^2}{dt} = k_1|A|^2 + k_2|A|^4, \quad (26)$$

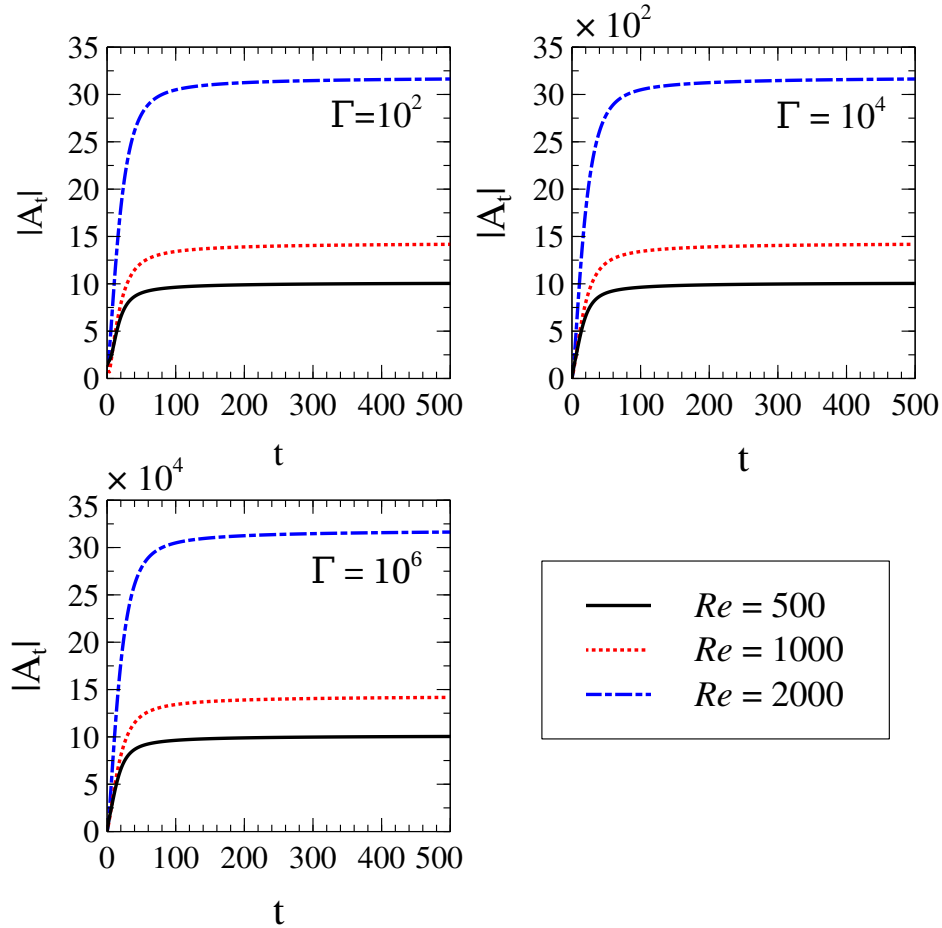


Fig. 5. Variation of $|A_t|$ as a function of t for three sets of Re and Γ with $k_y = k_z = 1$ for linear analysis in the Keplerian flow ($q = 1.5$).

where A is the amplitude of the nonlinear perturbations for the corresponding system, k_1 is $2\sigma_i$ and k_2 is the real part of $2p$, i.e., $2p_r$. Its solution is

$$|A|^2 = \frac{A_0^2}{-\frac{k_2}{k_1}A_0^2 + \left(1 + \frac{k_2}{k_1}A_0^2\right)e^{-k_1t}}, \quad (27)$$

where A_0 is the initial amplitude. Depending on the sign (positive/negative) of k_1 and k_2 , there are four^{21,23} different possible evolutions of $|A|$. These given below.

- In the present context of shear flows, k_1 (i.e., σ_i) is negative, but k_2 is positive. Therefore, there will be a threshold for initial amplitude A_i , determining the growth of perturbation. If the initial amplitude $A_0 < A_i$,

10

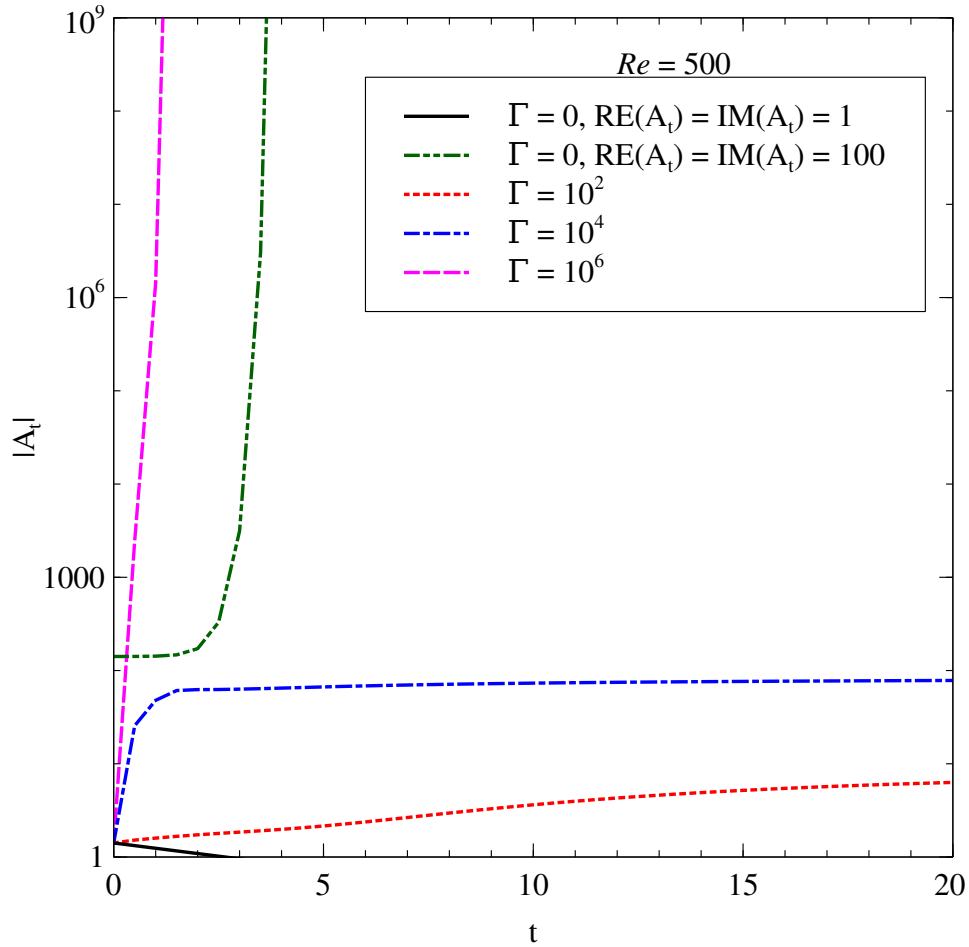


Fig. 6. Variation of $|A_t|$ as a function of t with $k_y = k_z = 1$ for nonlinear analysis in the Keplerian flow for $Re = 500$ and four different Γ . For $\Gamma \neq 0$, initial condition is $RE(A_t) = IM(A_t) = 1$.

then

$$|A|^2 \sim \frac{A_i^2 A_0^2 e^{k_1 t}}{A_i^2 - A_0^2} \quad (28)$$

at a large t . Therefore, $|A|^2 \rightarrow 0$ for $A_0 < A_i$ at $t \rightarrow \infty$. However, if $A_0 > A_i$, then $|A|^2 \rightarrow \infty$ at $t \rightarrow \ln(1 - A_i^2/A_0^2)/k_1$.

- If both k_1 and k_2 would be positive, $|A|^2$ blows up after a finite time. Hence, there will be a fast transition to turbulence.
- On the other hand, if $k_1 > 0$ but $k_2 < 0$, then $|A|^2 \rightarrow k_1/|k_2|$ at $t \rightarrow \infty$. In this case, $|A|^2$ at a large t does not depend on A_0 .
- Obviously, for k_1 and k_2 both negative, $|A|^2$ decays fast.

However, we have shown that the saturation in $|A_t|$ is $|\mathcal{N}|/|\sigma_i|$ in the linear regime. We have also argued that depending on Re and Γ , the system may already be in the nonlinear regime. The evolution of $|A_t|$ at the linear regime in our case, i.e., with extra force, is similar to that of $|A|$ from the equation (26), i.e. without force, for $k_1 > 0$ and $k_2 < 0$. In the Keplerian flow, k_1 , i.e. σ_i , is negative, but k_2 , i.e. p_r , could be positive. In the presence of extra force, the Landau equation modifies in such a way that the solution in the linear regime itself mimics the Landau equation without force (i.e., equation 26), however, with $k_1 > 0$ and $k_2 < 0$. Further, in the nonlinear regime, the amplitude A_t (i.e., with extra force included) diverges beyond a certain time, depending on Re and Γ . In the nonlinear regime, the Landau equation in the presence of extra force but negative k_1 (σ_i) is, therefore, mimicking the Landau equation without force but with positive k_1 and k_2 . Essentially, the extra force effectively changes the sign of k_1 (i.e., σ_i) for the Landau equation without force. Speaking in another way, the very presence of extra force destabilizes the otherwise stable system. Thus, the presence of force plays an important role in developing nonlinearity and turbulence in the case of Rayleigh stable flows.

Acknowledgment

S.G. acknowledges DST India for INSPIRE fellowship. This work is partly supported by a fund of Department of Science and Technology (DST-SERB) with research Grant No. DSTO/PPH/BMP/1946 (EMR/2017/001226).

References

1. N. I. Shakura and R. A. Sunyaev, Black holes in binary systems. Observational appearance, *Astronomy & Astrophysics* **24**, 337 (1973).
2. D. Lynden-Bell and J. E. Pringle, The Evolution of Viscous Discs and the Origin of the Nebular Variables, *Monthly Notices of the Royal Astronomical Society* **168**, 603 (09 1974).
3. S. A. Balbus and J. F. Hawley, A powerful local shear instability in weakly magnetized disks. I - Linear analysis. II - Nonlinear evolution, *The Astrophysical Journal* **376**, 214 (July 1991).
4. E. Velikhov, Stability of an ideally conducting liquid flowing between rotating cylinders in a magnetic field, *Zhur. Eksptl'. i Teoret. Fiz.* **36** (05 1959).
5. S. Chandrasekhar, The Stability of Non-Dissipative Couette Flow in Hydromagnetics, *Proceedings of the National Academy of Science* **46**, 253 (February 1960).
6. X.-N. Bai, Wind-driven Accretion in Protoplanetary Disks. II. Radial Dependence and Global Picture, *The Astrophysical Journal* **772**, p. 96 (Aug 2013).
7. M. E. Pessah and D. Psaltis, The Stability of Magnetized Rotating Plasmas with Superthermal Fields, *The Astrophysical Journal* **628**, 879 (August 2005).
8. U. Das, M. C. Begelman and G. Lesur, Instability in strongly magnetized accretion discs: A global perspective, *Monthly Notices of the Royal Astronomical Society* **473**, 2791 (2018).
9. S. K. Nath and B. Mukhopadhyay, Origin of nonlinearity and plausible turbulence by

- hydromagnetic transient growth in accretion disks: Faster growth rate than magnetorotational instability, *Physical Review E* **92**, p. 023005 (August 2015).
10. T. Singh Bhatia and B. Mukhopadhyay, Exploring non-normality in magnetohydrodynamic rotating shear flows: Application to astrophysical accretion disks, *Physical Review Fluids* **1**, p. 063101 (October 2016).
 11. S. K. Nath and B. Mukhopadhyay, A Pure Hydrodynamic Instability in Shear Flows and Its Application to Astrophysical Accretion Disks, *The Astrophysical Journal* **830**, p. 86 (October 2016).
 12. S. Ghosh and B. Mukhopadhyay, Hydrodynamical instability with noise in the Keplerian accretion discs: modified Landau equation, *Monthly Notices of the Royal Astronomical Society* **496**, 4191 (August 2020).
 13. B. Mukhopadhyay, N. Afshordi and R. Narayan, Bypass to Turbulence in Hydrodynamic Accretion Disks: An Eigenvalue Approach, *The Astrophysical Journal* **629**, 383 (August 2005).
 14. B. Mukhopadhyay, R. Mathew and S. Raha, Growing pseudo-eigenmodes and positive logarithmic norms in rotating shear flows, *New Journal of Physics* **13**, p. 023029 (February 2011).
 15. S. Ghosh and B. Mukhopadhyay, Forced linear shear flows with rotation: rotating couette-poiseuille flow, its stability and astrophysical implications (2021).
 16. Yecko, P. A., Accretion disk instability revisited - transient dynamics of rotating shear flow, *Astronomy & Astrophysics* **425**, 385 (2004).
 17. N. Afshordi, B. Mukhopadhyay and R. Narayan, Bypass to Turbulence in Hydrodynamic Accretion: Lagrangian Analysis of Energy Growth, *The Astrophysical Journal* **629**, 373 (August 2005).
 18. F. Rincon, G. I. Ogilvie and C. Cossu, On self-sustaining processes in Rayleigh-stable rotating plane Couette flows and subcritical transition to turbulence in accretion disks, *Astronomy & Astrophysics* **463**, 817 (Mar 2007).
 19. B. Mukhopadhyay and A. K. Chattopadhyay, Stochastically driven instability in rotating shear flows, *Journal of Physics A Mathematical General* **46**, p. 035501 (January 2013).
 20. T. Ellingsen, B. Gjevik and E. Palm, On the non-linear stability of plane Couette flow, *Journal of Fluid Mechanics* **40**, 97 (1970).
 21. P. Schmid, D. Henningson and D. Jankowski, Stability and Transition in Shear Flows. Applied Mathematical Sciences, *Applied Mechanics Reviews* **55**, p. B57 (2002).
 22. S. R. Rajesh, Weakly non-linear stability of a hydrodynamic accretion disc, *Monthly Notices of the Royal Astronomical Society* **414**, 691 (June 2011).
 23. P. G. Drazin and W. H. Reid, *Hydrodynamic Stability* September 2004.